Boron Clusters

Deutsche Ausgabe: DOI: 10.1002/ange.201703111
Internationale Ausgabe: DOI: 10.1002/anie.201703111

PrB_7^-: A Praseodymium-Doped Boron Cluster with a Pr^{II} Center Coordinated by a Doubly Aromatic Planar η^7-B_7^{3-} Ligand

Teng-Teng Chen[+], Wan-Lu Li[+], Tian Jian, Xin Chen, Jun Li, and Lai-Sheng Wang**

Abstract: *The structure and bonding of a Pr-doped boron cluster (PrB_7^-) are investigated using photoelectron spectroscopy and quantum chemistry. The adiabatic electron detachment energy of PrB_7^- is found to be low [1.47(8) eV]. A large energy gap is observed between the first and second detachment features, indicating a highly stable neutral PrB_7. Global minimum searches and comparison between experiment and theory show that PrB_7^- has a half-sandwich structure with C_{6v} symmetry. Chemical bonding analyses show that PrB_7^- can be viewed as a $Pr^{II}[\eta^7\text{-}B_7^{3-}]$ complex with three unpaired electrons, corresponding to a Pr ($4f^3 6s^1$) open-shell configuration. Upon detachment of the 6s electron, the neutral PrB_7 cluster is a highly stable $Pr^{III}[\eta^7\text{-}B_7^{3-}]$ complex with Pr in its favorite +3 oxidation state. The B_7^{3-} ligand is found to be highly stable and doubly aromatic with six delocalized π and six delocalized σ electrons and should exist for a series of lanthanide $M^{III}[\eta^7\text{-}B_7^{3-}]$ complexes.*

The electron deficiency of boron leads to electron sharing/delocalization in many boron compounds and the concepts of π and σ double aromaticity. Hoffmann and Berndt reviewed doubly aromatic boron compounds that contain a pair of both delocalized π and σ electrons over three boron centers.[1] In these compounds, both the delocalized electron systems (π and σ) satisfy the Hückel rule ($4N+2$) with $N=0$. The simplest such system is in fact the bare B_3^- cluster,[2] which contains three localized B–B bonds and a pair of delocalized π and σ bonds, making it the smallest doubly aromatic species. The B_3^+ cation is only π aromatic with three B–B bonds and a pair of delocalized π electrons.[3] Its complexes with CO and N_2 have been recently characterized using infrared spectroscopy.[4] The D_{3h} $B_3H_3^{2-}$ species is also π aromatic analogous to cyclopropenyl cation ($C_3H_3^+$)[5] and its more complicated $B_3R_3^{2-}$ analogue by substituting the H atoms with three bulky R ligands has been synthesized recently.[6] Here we report a lanthanide boron complex, PrB_7^-, which contains a doubly aromatic boron cluster with $N=1$ in both the π and σ systems, i.e., six delocalized π and six delocalized σ electrons.

Joint photoelectron spectroscopy (PES) and quantum chemistry studies over the past decade have shown that size-selected anionic boron clusters (B_n^-) are planar over a wide size range and their chemical bonding are dominated by multiple π and σ aromaticity.[7–10] The first cluster which was found to be doubly aromatic with $N=1$ was the B_9^- cluster,[11] which has a D_{8h} structure with six delocalized π and σ electrons, that has led to the design and observation of a series of borometallic doubly aromatic M©B_n^- clusters.[12] The bonding in B_8^{2-} observed in LiB_8^- (i.e. $Li^+[B_8^{2-}]$) is similar to that in B_9^- with double aromaticity for $N=1$.[13] The ground state of the B_7^- cluster was first found to be a triplet state with C_{6v} symmetry and doubly aromatic; its degenerate HOMO ($3e_1$) is half-filled and fulfills the Hückel rule ($4N$) for triplet-state aromaticity.[14] Thus, the B_7^{3-} species would be the smallest closed-shell boron cluster with double π and σ aromaticity with $N=1$. It was first observed in AlB_7^- {$Al^{II}[B_7^{3-}]$}, although the π aromaticity was disrupted in neutral AlB_7 because the first electron detachment occurred from the $3e_1$ (π) orbital on the B_7^{3-} moiety.[15]

The lanthanide elements have very low electronegativities and should be ideal to form $M^{III}[B_7^{3-}]$-type complexes with the smallest doubly aromatic boron cluster containing six delocalized π and σ electrons. Lanthanide borides represent a class of important magnetic, superconducting, and thermoelectric materials.[16] However, very few lanthanide doped-boron clusters have been investigated experimentally.[17] In the current article, we present a joint PES and ab initio study on the electronic structure and chemical bonding of the PrB_7^- cluster. The experiment was done with a magnetic-bottle type PES apparatus equipped with a laser vaporization supersonic cluster source and a time-of-flight mass spectrometer, details of which have been published elsewhere.[9,18] Briefly, the PrB_7^- cluster was generated by laser ablation of a Pr/^{11}B mixed target followed by supersonic expansion with a He carrier gas containing 5% argon. Various PrB_n^- clusters were produced (Figure S1 in the Supporting Information) and the PrB_7^- cluster of current interest was mass-selected and decelerated before photodetachment by the 193 nm (6.424 eV) radiation from an ArF excimer laser. The photoelectron spectrum was calibrated using the spectrum of Bi^-. The energy resolution of the apparatus was about 2.5%, that is, ca. 25 meV for 1 eV electrons.

The global minimum for PrB_7^- was investigated using the Tsinghua Global Minimum (TGMin) search program with a constraint Basin Hopping algorithm.[19] More than 400 trial structures for both doublet and quartet states were examined using the ADF 2016.101 software[20] with the PBE exchange-

[*] T. T. Chen,[+] T. Jian, Prof. Dr. L. S. Wang
Department of Chemistry, Brown University
Providence, RI 02912 (USA)
E-mail: Lai-Sheng_Wang@brown.edu
W. L. Li,[+] X. Chen, Prof. Dr. J. Li
Department of Chemistry and Key Laboratory of Organic Optoelectronics & Molecular Engineering of Ministry of Education, Tsinghua University
Beijing 100084 (China)
E-mail: junli@tsinghua.edu.cn
[+] These authors contributed equally to this work.
Supporting information and the ORCID identification number(s) for the author(s) of this article can be found under: https://doi.org/10.1002/anie.201703111.

correlation functional[21] and the TZP basis sets.[22] The frozen core approximation was employed for the inner shells, that is, [$1s^2$] for B and [$1s^2$-$4d^{10}$] for Pr. The scalar relativistic (SR) effects were taken into account by the zero-order-regular approximation (ZORA).[23] Calculations using the hybrid PBE0 functional[24] and TZP basis sets were further performed to determine the possible electronic states of the global minimum structure. Since two different electron configurations of Pr (f^2s^1 or f^3) were possible, single-point calculations at the CCSD(T) level were carried out for the two lowest energy isomers with these electron configurations using the corresponding PBE0/TZP optimized geometries. In the CCSD(T) calculations, the valence triple-ζ basis set (cc-pVTZ) was applied for B[25] and the Stuttgart energy-consistent relativistic pseudopotential ECP28MWB (Pr) with the corresponding ECP28MWB_ANO basis set was used for Pr.[26–28] The CCSD T1 diagnostic factors were calculated to be 0.026 and 0.037, indicating that the multi-configurational character was not significant for the PrB_7^- cluster.

Vertical detachment energies (VDEs) were calculated using the ΔSCF-TDDFT approach, as described before.[29] The first VDE (VDE_1) was calculated as the difference in energy between the anionic ground state and the corresponding neutral ground state at the anion geometry. Vertical excitation energies of the neutral species calculated using the time-dependent DFT method at the SAOP functional (TD-SAOP) level[30] were added to VDE_1 to yield the higher VDEs. The first adiabatic detachment energy (ADE), calculated only for the global minimum C_{6v} isomer, was obtained as the energy difference between the anionic and neutral species at their respective optimized geometries. The chemical bonding and orbital interactions were analyzed using the Kohn–Sham canonical molecular orbitals at the PBE0/TZP level and the adaptive natural density partitioning (AdNDP) method.[31]

The PE spectrum of PrB_7^- (Figure 1) shows a relatively simple pattern in the low binding energy region. There is a large energy gap between the ground state band X and the strong band A, beyond which the spectrum becomes more congested. The labels B to E are given only for the sake of discussion, because they may represent multiple detachment transitions. The lowest binding energy band X corresponds to detachment transition from the ground electronic state of PrB_7^- to that of PrB_7, while the higher binding energy bands from A to E denote detachment transitions to excited electronic states of neutral PrB_7. The band X gives rise to a VDE of 1.61 eV from the band maximum, and an ADE of 1.47(8) eV, which also represents the electron affinity (EA) of neutral PrB_7. The EA measured for PrB_7 is lower than that of B_7 or any known boron clusters,[9] indicating that the first electron detachment from PrB_7^- occurs from a Pr-based orbital. The spectral width of the X band indicates some geometry changes between the ground states of the anion and the neutral. Band A with a VDE of 3.15 eV is the most intense band and is also quite broad. The low ADE and the large gap between the X and A bands suggest that neutral PrB_7 is a highly stable electronic system. The experimental VDEs of all the observed PES bands are given in Table 1, as well as in Figure 1 as vertical bars (see below).

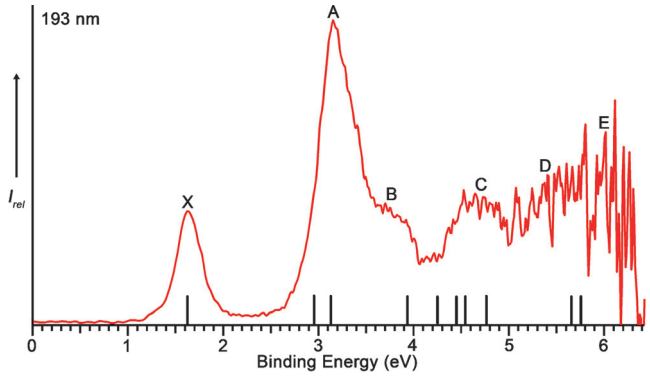

Figure 1. The photoelectron spectrum of PrB_7^- at 193 nm (6.424 eV). The vertical bars represent the calculated vertical detachment energies (see Table 1).

Table 1: Experimental vertical detachment energies (VDEs) for PrB_7^- compared with the calculated data at the ΔSCF-TDDFT level with the SAOP functional.

	VDE [eV] (expt.)	Final state and electron configuration	VDE [eV] (theor.)
X	1.61(6)	$^3B_1$, {...$4a_1^4 5a_1^2 1b_2^2 3e_1^4 4e_1^4 1b_1^1 6a_1^1$**$7a_1^0$**}	1.61
A	3.15(6)	$^5E_2$, {...$4a_1^4 5a_1^2 1b_2^2 3e_1^4$**$4e_1^3$**$1b_1^1 6a_1^1 7a_1^1$}	2.96
		$^3E_2$, {...$4a_1^4 5a_1^2 1b_2^2 3e_1^4$**$4e_1^3$**$1b_1^1 6a_1^1 7a_1^1$}	3.11
B	≈3.8	$^3B_1$, {...$4a_1^4 5a_1^2 1b_2^2 3e_1^4 4e_1^4 1b_1^1$**$6a_1^0$**$7a_1^1$}	3.93
		$^3A_1$, {...$4a_1^4 5a_1^2 1b_2^2 3e_1^4 4e_1^4$**$1b_1^0$**$6a_1^1 7a_1^1$}	4.26
C	≈4.7	$^5E_2$, {...$4a_1^4 5a_1^2 1b_2^2$**$3e_1^3$**$4e_1^4 1b_1^1 6a_1^1 7a_1^1$}	4.45
		$^3E_2$, {...$4a_1^4 5a_1^2 1b_2^2$**$3e_1^3$**$4e_1^4 1b_1^1 6a_1^1 7a_1^1$}	4.54
		$^5A_2$, {...$4a_1^4 5a_1^2$**$1b_2^1$**$3e_1^4 4e_1^4 1b_1^1 6a_1^1 7a_1^1$}	4.79
		$^3A_2$, {...$4a_1^4 5a_1^2$**$1b_2^1$**$3e_1^4 4e_1^4 1b_1^1 6a_1^1 7a_1^1$}	4.79
D	≈5.4	$^5B_1$, {...$4a_1^4$**$5a_1^1$**$1b_2^2 3e_1^4 4e_1^4 1b_1^1 6a_1^1 7a_1^1$}	5.68
E	≈6.0	$^3B_1$, {...$4a_1^4$**$5a_1^1$**$1b_2^2 3e_1^4 4e_1^4 1b_1^1 6a_1^1 7a_1^1$}	5.76

The optimized structures within 80 kcal mol^{-1} of the global minimum at the PBE/TZP level are given in Figure S2. The global minimum of PrB_7^- was found to have C_{6v} symmetry with a high-spin electronic state ($^4B_1$), both at the PBE/TZP and PBE0/TZP levels. The low-spin doublet state ($^2A_1$) with the same electron configuration of the C_{6v} structure lies ≈5 kcal mol^{-1} higher in energy at the PBE/TZP level. All other structures are much higher in energy, indicating the overwhelming stability of the C_{6v} half-sandwich-type structure for PrB_7^-. Due to the strong electron correlation effects among the $4f^36s^0$, $4f^26s^1$, $4f^1(6s5d)^2$ configurations on Pr, total energies of a number of different electron configurations were determined initially at the PBE/TZP level (Table S1). Isomers with the $4f^26s^1$ configuration were found to be much more stable than those with $4f^3$. Thus, the global minimum C_{6v} structure has three unpaired electrons on Pr ($4f\phi^1 4f\sigma^1 6s^1$, $^4B_1$), revealing an uncommon Pr^{II} oxidation state. On the other hand, the different configurations of bare Pr^{2+} have the following order: $4f^36s^0$ (0.0 eV) < $4f^25d^1$ (1.66 eV) < $4f^26s^1$ (3.52 eV).[32] The Pr $4f^26s^1$ configuration in PrB_7^- is reminiscent of the U $5f^27s^1$ configuration in UO_2^-.[33] The preference of occupying the ns orbitals rather than the $(n-2)$f orbitals in

low-oxidation state f-element complexes is due to the more penetrating and diffuse feature of the radial probability distribution of the *ns* orbitals.[34] The energy gap between the two lowest $4f^26s^1$ and $4f^3$ states (***a*** and ***e*** in Table S1) is calculated to be 9.44 kcal mol^{-1} at the PBE/TZP level or 13.59 kcal mol^{-1} at the CCSD(T) level.

The VDE_1 and ADE computed at two levels of theory are compared with the measured value in Table S2. The higher VDEs are obtained by adding the TDDFT excitation energies to VDE_1. The calculated VDE_1 from PBE and PBE0 are both ca. 0.1 eV lower than the measured value. To facilitate comparison with the experimental data, the computed VDEs in Table 1 are all shifted by aligning the VDE_1 to match the X band. The Kohn–Sham molecular orbital (MO) levels of PrB_7^- are shown in Figure 2, where the isosurfaces of the five frontier MOs are also displayed. The pictures of all valence MOs are plotted in Figure S3. The MOs associated with the B_7 moiety are all lower in energy than the Pr-derived MOs, ranging from $4e_1$ to $3a_1$. The Pr 4f-based orbitals ($1b_1$ and $6a_1$) are only slightly above the boron-based MOs, while the Pr 6s-based orbital ($7a_1$) lies much higher in energy, because of the antibonding interactions with the boron orbitals. The first electron detachment corresponds to removal of the $6s^1$ electron from the highest singly occupied molecular orbital (SOMO, $7a_1$), giving rise to the final triplet state $^3B_1$ with a Pr^{III} oxidation state. The calculated VDE_1 values at PBE (1.52 eV) and PBE0 (1.54 eV) are in good agreement with the experimental value of 1.61 eV for band X. The first ADE calculated at PBE (1.43 eV) and PBE0 (1.45 eV) also agree well with the experimental value of 1.47 eV (Table S2).

The next band A is derived from electron detachment from a deeper boron-based bonding $4e_1$ orbital (HOMO), rather than the next two SOMO−1 ($6a_1$) and SOMO−2 ($1b_1$) of Pr 4f character. This breakdown of the Koopmans' theorem is common in strongly correlated f-element systems.[33,35] The more contracted Pr 4f orbitals are significantly stabilized upon electron detachment, so that the $(4e_1)^3(4f)^2(6s)^1$ configuration becomes energetically more favorable than $(4e_1)^4(4f)^1(6s)^1$ in neutral PrB_7. This trend of f-orbitals being increasingly more stabilized upon electron ionization is also observed in other 4f and 5f systems.[36] The electron detachment from the $4e_1$ HOMO orbital leads to two final states, $^5E_2$ (VDE: 2.96 eV) and $^3E_2$ (VDE: 3.11 eV). The theoretical VDEs from these two final states agree well with the observed VDE of 3.15 eV for band A. Beyond band A, the PE spectrum becomes congested and less well resolved, in agreement with multiple detachment channels from both the Pr 4f SOMOs and the deeper bonding orbitals from the B_7 moiety (Figure 1 and Table 1). Overall, the theoretical results are in good agreement with the experimental data, providing considerable credence to the C_{6v} global minimum for PrB_7^- and its high-spin state.

The optimized C_{6v} structures for PrB_7^- and neutral PrB_7 at the PBE0/TZP level are shown in Figure 3 and the corresponding coordinates are listed in Table S4. The PrB_7^- anion

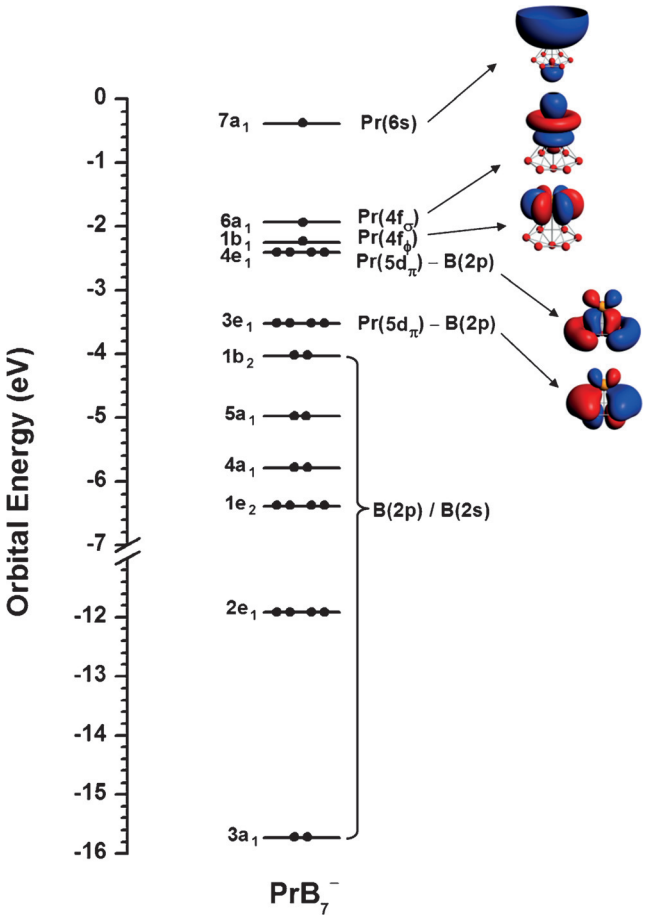

Figure 2. The Kohn–Sham molecular orbital energy levels of PrB_7^- at the PBE0/TZP level.

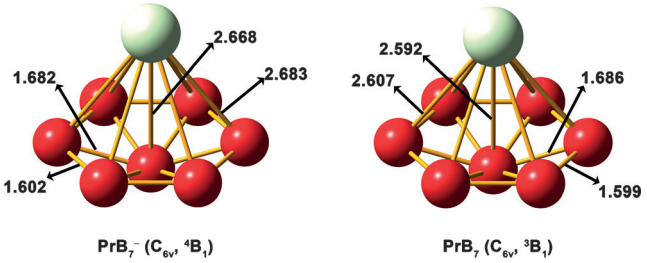

Figure 3. The optimized global minimum structures of PrB_7^- and neutral PrB_7. The bond lengths are given in Å.

can be viewed as $Pr^{II}(\eta^7\text{-}B_7^{3-})$, whereas neutral PrB_7 can be viewed as $Pr^{III}(\eta^7\text{-}B_7^{3-})$. The low binding energy of the $6s^1$ ($7a_1$) electron and the large X–A gap revealed in the PE spectrum of PrB_7^- (Figure 1) suggest that neutral PrB_7 is a much more stable molecule, in which Pr is in its favorite +3 oxidation state. The major structural changes between the PrB_7^- anion and its neutral are the Pr–B distances, which become significantly shorter, in agreement with stronger Pr–B_7 bonding and a more stable PrB_7 neutral complex.[37] This geometry change upon oxidation from Pr^{II} to Pr^{III} is also in agreement with the relatively broad feature of the PES band X (Figure 1). However, there is little geometry change in the B_7^{3-} moiety between the anionic and neutral PrB_7. The calculated Mulliken charges and spin densities of the Pr and B atoms in PrB_7 and PrB_7^- are given in Table S3. The Pr and the

central B atom are both positively charged, which lose electron density to the B_6 ring. The spin density distributions agree with the Pr^{III} and Pr^{II} oxidation states in PrB_7 and PrB_7^-, respectively. Previous calculations on FeB_7 and ScB_7 found similar C_{6v} structures as PrB_7.[38,39] However, joint PES and theoretical study on TaB_7^- revealed that it has a C_s structure, in which the B_7 moiety is distorted to optimize bonding with the Ta center.[40]

To further understand the chemical bonding in $Pr(\eta^7\text{-}B_7)^-$ and $Pr(\eta^7\text{-}B_7)$, we can examine the MOs in the anion (Figure S3). There are three unpaired electrons in SOMO ($7a_1$), SOMO−1 ($6a_1$) and SOMO−2 ($1b_1$) in PrB_7^-. The SOMO ($7a_1$) is mainly from the Pr 6s orbital with some contribution from the Pr $6p_z$ orbital. The SOMO−1 ($6a_1$) and SOMO−2 ($1b_1$) are basically from the Pr 4fσ and 4fϕ orbitals, respectively. The remaining twelve occupied MOs from $4e_1$ down to $3a_1$ essentially describe the bonding in the B_7^{3-} ligand with relatively small bonding contributions from the Pr center. In fact, these MOs look very similar to those in the bare C_{6v} B_7^- cluster, in which the HOMO e_1 orbital is half-filled.[14] With the exception of the weak 5dπ contributions, these orbitals are identical to those in the C_{6v} AlB_7^-,[15] which can be viewed as $Al^{II}(B_7^{3-})$, albeit neutral AlB$_7$ [$Al^{II}(B_7^{2-})$] is quite different from PrB_7.

The bonding in the B_7^{3-} moiety can be better appreciated from the AdNDP analyses (Figure 4).[31] We see clearly six two-center two-electron (2c-2e) bonds around the peripheral B atoms of the B_7^{3-} ligand. Of particular importance are the two sets of multi-center bonds: three in-plane seven-center two-electron (7c–2e) bonds and three out-of-plane eight-center two-electron (8c–2e) bonds, which represent the π bonding within B_7^{3-} and bonding interactions between the Pr 5dπ orbitals and the B_7^{3-} ligand. The delocalized σ and π bonds in B_7^{3-} are reminiscent of the σ and π bonds in both B_8^{2-} and B_9^-,[11] giving rise to double aromaticity. Both the σ and π bonds fulfill the Hückel $4N+2$ rule with $N=1$. The C_{6v} symmetry of B_7^{3-} and also in B_7^- is due to the fact that the B_6 ring is too small to fit the central B atom perfectly.[41] In fact, the slight bowl-shape of B_7^{3-} makes it a more suitable ligand to form half-sandwich complexes than the perfect planar B_8^{2-} and B_9^- species.

In conclusion, we report an investigation of a Pr-doped B_7^- cluster using photoelectron spectroscopy and quantum chemical calculations. We found that the global minimum of the PrB_7^- cluster is a C_{6v} half-sandwich structure with a Pr^{II} center coordinated by a $\eta^7\text{-}B_7^{3-}$ ligand. We observed that the extra electron in PrB_7^- is in a Pr 6s orbital and can be easily detached to produce a highly stable $Pr(\eta^7\text{-}B_7)$ neutral complex, in which the Pr is in its favorite +3 oxidation state with two unpaired 4f electrons. The B_7^{3-} ligand, which possesses double aromaticity with six delocalized π and σ electrons, is found to be nearly identical in both the PrB_7^- anion and its neutral. The Pr–$(\eta^7\text{-}B_7)$ ligand bonding is significantly enhanced, making it a viable candidate for possible chemical synthesis. Since all 4f elements prefer the +3 oxidation state, we expect that a whole series of lanthanide $M^{III}[\eta^7\text{-}B_7^{3-}]$ complexes exist, with tunable magnetic and optical properties.

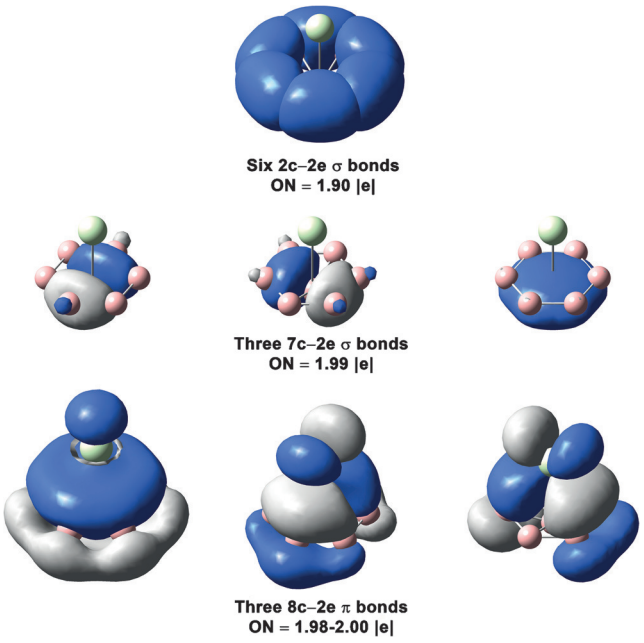

Figure 4. AdNDP analyses of the chemical bonding of the B_7^{3-} moiety in PrB_7 {$Pr^{III}[\eta^7\text{-}B_7^{3-}]$} at the PBE0/TZP level. The two unpaired and localized 4f electrons on Pr^{III} are not shown.

Acknowledgements

The experimental work at Brown University was supported by the National Science Foundation (CHE-1632813). The theoretical work at Tsinghua University was supported by NSFC (Grant Nos. 21590792, 91426302 and 21433005) of China. The calculations were performed using supercomputers at Tsinghua National Laboratory for Information Science and Technology, and the Supercomputing Center, Computer Network Information Center of the Chinese Academy of Sciences. T.J. thanks the Chemistry Department of Brown University for the Vince Wernig Fellowship.

Conflict of interest

The authors declare no conflict of interest.

Keywords: ab initio calculation · aromaticity · boron clusters · metal–boron cluster complex · photoelectron spectroscopy

How to cite: *Angew. Chem. Int. Ed.* **2017**, *56*, 6916–6920
Angew. Chem. **2017**, *129*, 7020–7024

[1] M. Hofmann, A. Berndt, *Heteroat. Chem.* **2006**, *17*, 224–237.
[2] Z. H. Zhai, L. S. Wang, A. N. Alexandrova, A. I. Boldyrev, V. G. Zakrzewski, *J. Phys. Chem. A* **2003**, *107*, 9319–9328.
[3] D. Y. Zubarev, A. I. Boldyrev, *J. Comput. Chem.* **2007**, *28*, 251–268.
[4] J. Jin, G. J. Wang, M. F. Zhou, D. M. Andrada, M. Hermann, G. Frenking, *Angew. Chem. Int. Ed.* **2016**, *55*, 2078–2082; *Angew. Chem.* **2016**, *128*, 2118–2122.

[5] A. A. Korkin, P. v. R. Schleyer, M. L. McKee, *Inorg. Chem.* **1995**, *34*, 961 – 977.
[6] T. Kupfer, H. Braunschweig, K. Radacki, *Angew. Chem. Int. Ed.* **2015**, *54*, 15084 – 15088; *Angew. Chem.* **2015**, *127*, 15299 – 15303.
[7] A. N. Alexandrova, A. I. Boldyrev, H. J. Zhai, L. S. Wang, *Coord. Chem. Rev.* **2006**, *250*, 2811 – 2866.
[8] A. P. Sergeeva, I. A. Popov, Z. A. Piazza, L. W. Li, C. Romanescu, L. S. Wang, A. I. Boldyrev, *Acc. Chem. Res.* **2014**, *47*, 1349 – 1358.
[9] L. S. Wang, *Int. Rev. Phys. Chem.* **2016**, *35*, 69 – 142.
[10] A. I. Boldyrev, L. S. Wang, *Phys. Chem. Chem. Phys.* **2016**, *18*, 11589 – 11605.
[11] a) H. J. Zhai, A. N. Alexandrova, K. A. Birch, A. I. Boldyrev, L. S. Wang, *Angew. Chem. Int. Ed.* **2003**, *42*, 6004 – 6008; *Angew. Chem.* **2003**, *115*, 6186 – 6190; b) L. L. Pan, J. Li, L. S. Wang, *J. Chem. Phys.* **2008**, *129*, 024302.
[12] C. Romanescu, T. R. Galeev, L. W. Li, A. I. Boldyrev, L. S. Wang, *Acc. Chem. Res.* **2013**, *46*, 350 – 358.
[13] A. N. Alexandrova, H. J. Zhai, L. S. Wang, A. I. Boldyrev, *Inorg. Chem.* **2004**, *43*, 3552 – 3554.
[14] A. N. Alexandrova, A. I. Boldyrev, H. J. Zhai, L. S. Wang, *J. Phys. Chem. A* **2004**, *108*, 3509 – 3517.
[15] T. R. Galeev, C. Romanescu, W. L. Li, L. S. Wang, A. I. Boldyrev, *J. Chem. Phys.* **2011**, *135*, 104301.
[16] a) P. Shankhari, P. R. N. Misse, M. Mbarki, H. Park, B. P. T. Fokwa, *Inorg. Chem.* **2017**, *56*, 446 – 451; b) B. P. T. Fokwa, *Eur. J. Inorg. Chem.* **2010**, 3075 – 3092; c) "Lanthanides: Boride, Carbide, and Nitride Compounds": T Mori, in *Encyclopedia of Inorganic and Bioinorganic Chemistry*, Wiley, Hoboken, **2012**.
[17] a) S. B. Cheng, C. Berkdemir, A. W. Castleman, *Phys. Chem. Chem. Phys.* **2014**, *16*, 533 – 539; b) P. J. Robinson, X. Zhang, T. McQueen, K. H. Bowen, A. N. Alexandrova, *J. Phys. Chem. A* **2017**, *121*, 1849 – 1854.
[18] L. S. Wang, H. S. Cheng, J. Fan, *J. Chem. Phys.* **1995**, *102*, 9480 – 9493.
[19] a) X. Chen, Y. F. Zhao, L. S. Wang, J. Li, *Comput. Theor. Chem.* **2017**, *1107*, 57 – 65; b) Y. F. Zhao, X. Chen, J. Li, *Nano Res.* **2017**, https://doi.org/10.1002/s12274-017-1553-z.
[20] ADF, 2016.101, SCM, Theoretical Chemistry, Vrijie Universiteit, Amsterdam, The Netherlands, (http://www.scm.com).
[21] J. P. Perdew, K. Burke, M. Ernzerhof, *Phys. Rev. Lett.* **1996**, *77*, 3865 – 3868.
[22] E. van Lenthe, E. J. Baerends, *J. Comput. Chem.* **2003**, *24*, 1142 – 1156.
[23] E. van Lenthe, E. J. Baerends, J. G. Snijders, *J. Chem. Phys.* **1993**, *99*, 4597 – 4610.
[24] C. Adamo, V. Barone, *J. Chem. Phys.* **1999**, *110*, 6158 – 6170.
[25] T. H. Dunning, Jr., *J. Chem. Phys.* **1989**, *90*, 1007 – 1023.
[26] M. Dolg, H. Stoll, H. Preuss, *J. Chem. Phys.* **1989**, *90*, 1730 – 1734.
[27] X. Cao, M. Dolg, *Chem. Phys. Lett.* **2001**, *349*, 489 – 495.
[28] X. Cao, M. Dolg, *J. Chem. Phys.* **2001**, *115*, 7348 – 7355.
[29] a) J. Li, X. Li, H. J. Zhai, L. S. Wang, *Science* **2003**, *299*, 864 – 867; b) X. Li, B. Kiran, J. Li, H. J. Zhai, L. S. Wang, *Angew. Chem. Int. Ed.* **2002**, *41*, 4786 – 4789; *Angew. Chem.* **2002**, *114*, 4980 – 4983.
[30] P. R. T. Schipper, O. V. Gritsenko, S. J. A. v. Gisbergen, E. J. Baerends, *J. Chem. Phys.* **2000**, *112*, 1344 – 1352.
[31] D. Y. Zubarev, A. I. Boldyrev, *Phys. Chem. Chem. Phys.* **2008**, *10*, 5207 – 5217.
[32] J. Marçalo, J. K. Gibson, in *Handbook on the Physics and Chemistry of Rare Earths*, *Vol. 45* (Eds.: G. B. Jean-Claude, K. P. Vitalij), Elsevier, Amsterdam, **2014**, pp. 1 – 110.
[33] W. L. Li, J. Su, T. Jian, G. V. Lopez, H. S. Hu, G. J. Cao, J. Li, L. S. Wang, *J. Chem. Phys.* **2014**, *140*, 094306.
[34] J. B. Liu, G. P. Chen, W. Huang, D. L. Clark, W. H. E. Schwarz, J. Li, *Dalton Trans.* **2017**, *46*, 2542 – 2550.
[35] J. Su, W. L. Li, G. V. Lopez, T. Jian, G. J. Cao, W. L. Li, W. H. E. Schwarz, L. S. Wang, J. Li, *J. Phys. Chem. A* **2016**, *120*, 1084 – 1096.
[36] W. Huang, W. H. Xu, W. H. E. Schwarz, J. Li, *Inorg. Chem.* **2016**, *55*, 4616 – 4625.
[37] At the PBE/TZP level, the calculated binding energy between Pr and B_7 is 141.9 kcal mol^{-1} for PrB_7, while the binding energy between Pr and B_7^- is 111.3 kcal mol^{-1} in PrB_7^-.
[38] Z. Yang, S. J. Xiong, *J. Chem. Phys.* **2008**, *128*, 184310.
[39] J. Jia, L. Ma, J. F. Wang, H. S. Wu, *J. Mol. Model.* **2013**, *19*, 3255 – 3261.
[40] W. L. Li, A. S. Ivanov, J. Federič, C. Romanescu, I. Černušák, A. I. Boldyrev, L. S. Wang, *J. Chem. Phys.* **2013**, *139*, 104312.
[41] C. Romanescu, A. P. Sergeeva, W. L. Li, A. I. Boldyrev, L. S. Wang, *J. Am. Chem. Soc.* **2011**, *133*, 8646 – 8653.

Manuscript received: March 25, 2017
Version of record online: May 8, 2017

